Filomat 29:10 (2015), 2447–2455
DOI 10.2298/FIL1510447L

Published by Faculty of Sciences and Mathematics,
University of Niš, Serbia
Available at: http://www.pmf.ni.ac.rs/filomat

Form-Finding Software and Minimal Surface Equation: a Comparative Approach

Jana A. Lipkovski[a], Aleksandar T. Lipkovski[b]

[a]*Faculty of Architecture, University of Belgrade*
[b]*Faculty of Mathematics, University of Belgrade*

Abstract. The shape of membrane and cable-net structures is usually modeled by geometry of minimal surfaces. Using central finite differences method, a nonlinear iterative process for finding the minimal surface with given fixed boundary conditions is developed and implemented in Mathematica®. Having in mind form-finding of membrane structures, the results are compared with the results obtained by commercial package EASY®, made by Technet GmbH, Germany.

1. Introduction

Membrane structures are undoubtedly the most appropriate way to cover large areas or objects, without thermal insulation demands. Minimal use of building materials is an invincible argument in their favor, primarily during the lasting financial crisis. Unfortunately, in the region of South-Eastern Europe, there are almost none representative projects of tensile structures. Due to the lack of knowledge of domestic architects and engineers in this field, many investors and developers habitually use "classical" stiff construction forms, even if all indications of the project task are in favor of membrane or other tensile structural systems (eg. cable-nets). Worldwide, tensile structures are treated completely equally to all other structure types and there are several methods, that have been developed for form-finding and structural analysis of membranes and cable-nets. Veenendaal and Block in [6] give an overview of the methods commonly used for form-finding of membranes and cable-nets.

The shape of membrane and cable-net structures corresponds to the geometry of minimal surfaces, which is a double curved surface that occupies the smallest area under certain boundary conditions - a particular form of boundary curves. The membrane and cable-net structures are, like the soap-film, evenly tensioned in all directions.

The experiments with minimal surfaces and soap films and their application in architecture have been studied since 1960's by German engineers Frei Otto and Bodo Rasch, at the University of Stuttgart, Institute

2010 *Mathematics Subject Classification*. Primary 53-04; Secondary 53A10
Keywords. form-finding, membrane structure, tensile structure, minimal surface, Laplace equation, force-density method, Mathematica®
Received: 01 July 2015; Accepted: 22 July 2015
Communicated by Lj. Velimirovic
The first author expresses her sincere gratitude to Jürgen Holl and Bernd Stary from Technet GmbH for time-limited free use of the software package EASY®. The second author acknowledges the support of the Ministry of Education, Science and Technical Development of the Republic of Serbia under grant OI 174020.
Email addresses: j.lipkovski@gmx.de (Jana A. Lipkovski), acal@matf.bg.ac.rs (Aleksandar T. Lipkovski)

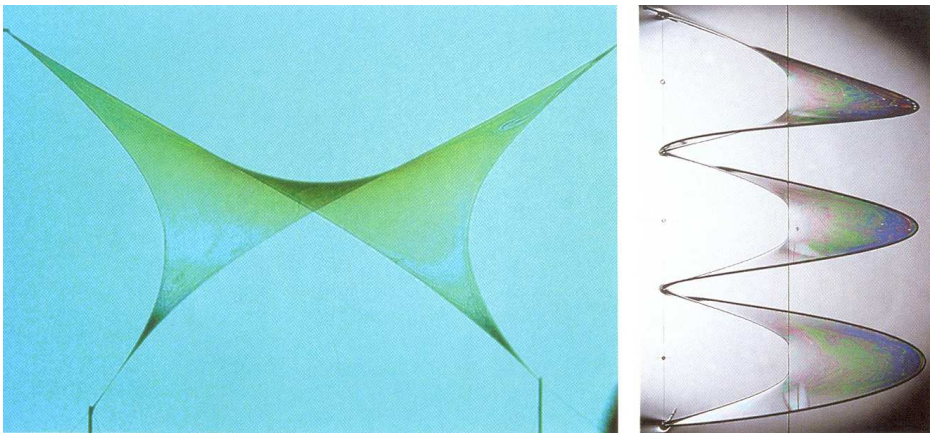

Figure 1: Soap film experiments (Otto,Rasch [3])

for Lightweight Structures (former IL, today ILEK). The experiments were documented very detailed in [5] (*Fig. 1*).

As a result of these experimental research a few experimental buildings were built, like the building of the Institute in Vaihingen – Stuttgart, Germany – a cable-net tent-like structure.

The experimental form finding methods reached their limits very fast – though they were crucial for the understanding of a complete new approach in architecture: "Form follows force". Without the experimental form finding, it would be almost impossible to define the form, which would meet the structural ideal – the minimal surface.

The apparatus for experimenting with physical models was rather complicated, and the preservation was an issue. Also, further calculation on the "found" initial form was almost impossible. It was necessary to make very expensive and complicated measuring models to make a prediction of the structural behavior of the construction. For these reasons, a few multidisciplinary groups of engineers in Germany, Great Britain and USA made the effort on formulating mathematical methods that would offer a faster and easier way to generate initial structural forms that could be used for further structural analysis and could be implemented in commercial software and would simulate the soap-film form generation.

There are several research and commercial program packages for form-finding purposes. However, due to differences in their mathematical background and solution methods, the results may vary. For a comprehensive review of various methods, see [6]. In [7], a visual comparison of the results of different form finding methods for the IL building in Stuttgart has been given.

A soap film over a closed boundary curve is from the mathematical point of view a minimal surface that can be described in various theoretical mathematical settings: variational, differential-geometric, complex analytic etc. The classical textbook on this matter is [1].

2. Solution by Force-density Method

Software which has been used for form-finding in the present work is based on the Force Density Method. The method has been developed by Linkwitz and Schek in 1971 in the University of Stuttgart. A detailed description of the software package can be found in [9]. Here we give a brief explanation of the method.

The initial point for all form finding methods is the net structure of nodes and branches whose topology is described by matrix **C,** *branch-node matrix* or *Kanten-Knoten-Matrix*. It is analogous to the incidence matrix in graph theory. Nodes can be of two types: fixed (boundary) and free (interior).

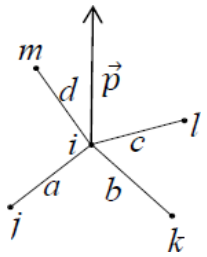

Figure 2: A single node i of the network in the state of equilibrium

Nodes' coordinates form a coordinate vector **x**, and the product **u** = **Cx** represents the branches' coordinate vector, obtained as differences of coordinates of the branch ends for every rod. Branch lengths are obtained as $l = (\mathbf{u}^T\mathbf{u})^{1/2}$. We use the standard notational convention: small bold letters denote vectors, and capital bold letters denote corresponding diagonal matrices. Total matrices of the cable network which contain coordinates of nodes, branches and their lengths will be denoted by **X, U** and **L,** respectively. For more details, see [11].

The network is in the state of equilibrium, if in each node inner forces are balanced with external loads **p**. For a single node, it is represented on the following figure:

For a chosen node i in the network, let j, k, l, m be its neighbouring nodes, a, b, c, d branches determined by pairs of nodes $i-j$, $i-k$, $i-l$, $i-m$ respectively. The force equilibrium is expressed by the equation:

$$\overrightarrow{f_a} + \overrightarrow{f_b} + \overrightarrow{f_c} + \overrightarrow{f_d} = \overrightarrow{p} \tag{1}$$

If we notice that

$$\overrightarrow{f_a} = f_a \cdot \frac{\overrightarrow{u_a}}{l_a} \tag{2}$$

where

$$\overrightarrow{u_a} = \frac{\mathbf{u}_a}{l_a} \tag{3}$$

and

$$\overrightarrow{u_a} = \left(x_j - x_i\right)\overrightarrow{i} + \left(y_j - y_i\right)\overrightarrow{j} + \left(z_j - z_i\right)\overrightarrow{k} \tag{4}$$

and $\overrightarrow{u_a}/l_a$ is the unit vector of the branch a, we can write the equation of the equilibrium in the form

$$q_a\overrightarrow{u_a} + q_b\overrightarrow{u_b} + q_c\overrightarrow{u_c} + q_d\overrightarrow{u_d} = \overrightarrow{p} \tag{5}$$

where the new quantities $q_a = f_a/l_a$, $q_b = f_b/l_b$, $q_c = f_c/l_c$, $q_d = f_d/l_d$ form a vector **q.** This quantity represents the force on the unit length of the branch, known as the force density (Schek [11]), or stress coefficient (Barnes [12]). This equation of the equilibrium has vector character and splits into three scalar equations

$$\begin{aligned}
&q_a\frac{x_j - x_i}{\sqrt{\left(x_j - x_i\right)^2 + \left(y_j - y_i\right)^2 + \left(z_j - z_i\right)^2}} + q_b\frac{x_k - x_i}{\sqrt{(x_k - x_i)^2 + (y_k - y_i)^2 + (z_k - z_i)^2}} + \\
&+q_c\frac{x_l - x_i}{\sqrt{(x_l - x_i)^2 + (y_l - y_i)^2 + (z_l - z_i)^2}} + q_d\frac{x_m - x_i}{\sqrt{(x_m - x_i)^2 + (y_m - y_i)^2 + (z_m - z_i)^2}} = p_x \\
&q_a\frac{y_j - y_i}{l_a} + q_b\frac{y_k - y_i}{l_b} + q_c\frac{y_l - y_i}{l_c} + q_d\frac{y_m - y_i}{l_d} = p_y \\
&q_a\frac{z_j - z_i}{l_a} + q_b\frac{z_k - z_i}{l_b} + q_c\frac{z_l - z_i}{l_c} + q_d\frac{z_m - z_i}{l_d} = p_z
\end{aligned} \tag{6}$$

These equations are not linear, since there are squares of the coordinates of the nodes a, b, c, d in the denominators.

The equilibrium equation of the whole cable network can be written in the following form:

$$\mathbf{P}_i - \mathbf{C}_i{}^T \mathbf{g}(u) = 0 \tag{7}$$

Here,$\mathbf{P}_i$ contains the vectors of external forces in all interior nodes, and $\mathbf{C}_i{}^T$ represents the vector of internal equivalent nodal forces for the whole network. Applying Taylor expansion to the second term, the system is linearized. One arrives at linear system with indeterminate coordinates of the interior nodes

$$\mathbf{K}_T \Delta x = \mathbf{r} \tag{8}$$

where

$$\mathbf{K}_T = \mathbf{C}_i^T \left(\frac{\partial \mathbf{g}(\mathbf{u})}{\partial \mathbf{u}} \right)_{\mathbf{u}^i = \mathbf{u}_0} \tag{9}$$

is the tangential stiffness matrix of the cable network, and $\mathbf{r}(\mathbf{u}) = \mathbf{r}(\mathbf{x})$ is non-balanced load in the network nodes in arbitrary iteration step. Vector $\mathbf{u} = \mathbf{u}_0$ contains branch coordinates of the preceding equilibrium state of the network.

System in *Eq. 8* leads to an iterative process

$$\mathbf{K}_T^{(i)} \Delta \mathbf{x}^{(i+1)} = \mathbf{r}^{(i)} \tag{10}$$

and the iteration is continued until the residual load is zero $\mathbf{r}^{(i)} = 0$ up to a certain given precision, which leads to equilibrium state in all nodes of the cable network.

The system is usually solved by standard or modified Newton-Raphson iterative method.

3. Direct Non-linear Iterative Solution for Minimal Surface Problem

For the purposes of this work, we use the explicit 2-variable formulation of the problem as second order quasi-linear partial differential equation with boundary condition, arising from the Euler-Lagrange area-minimizing condition. For a given open domain $U \subset \mathbb{R}^2$ with compact boundary $B = \partial U$ we are looking for a function $z = f(x, y) : U \to \mathbb{R}$ which satisfies the equation

$$\left(1 + f_x^2\right) f_{yy} + \left(1 + f_y^2\right) f_{xx} - 2 f_x f_y f_{xy} = 0. \tag{11}$$

Here, standard notation for partial derivatives ($f_x = \frac{\partial f}{\partial x}$ etc.) is used.

As a model example, we take a rectangular domain $U = (a, b) \times (c, d)$ bounded by a rectangle $B = \{a\} \times (c, d) \cup \{b\} \times (c, d) \cup (a, b) \times \{c\} \cup (a, b) \times \{d\}$. We use equidistant rectangular mesh with $n + 1$ points along x-axis and $m + 1$ points along y-axis, with steps h and k respectively, division points $x_i = a + ih$, $y_j = c + jk$ and mesh knots $P_{ij} = P_{ij}\left(x_i, y_j\right)$ $(i = 0, \ldots, n,\ j = 0, \ldots, m)$.

For discretization purposes we use central finite differences – a common approximation method. Approximations of partial derivatives in the inner points of the mesh are:

$$\begin{aligned}
f_x\left(P_{ij}\right) &\approx \frac{1}{2h}\left(f_{i+1,j} - f_{i-1,j}\right) \\
f_y\left(P_{ij}\right) &\approx \frac{1}{2k}\left(f_{i,j+1} - f_{i,j-1}\right) \\
f_{xx}\left(P_{ij}\right) &\approx \frac{1}{h^2}\left(f_{i+1,j} - 2f_{i,j} + f_{i-1,j}\right) \\
f_{yy}\left(P_{ij}\right) &\approx \frac{1}{k^2}\left(f_{i,j+1} - 2f_{i,j} + f_{i,j-1}\right) \\
f_{xy}\left(P_{ij}\right) &\approx \frac{1}{4hk}\left(f_{i+1,j+1} - f_{i-1,j+1} - f_{i+1,j-1} + f_{i-1,??-1}\right)
\end{aligned} \tag{12}$$

where the subscripts represent the values of the function f in mesh points $f_{i,j} = f\left(P_{ij}\right) = f\left(x_i, y_j\right)$. The approximation error has second order with respect to h, k. This gives rise to a system of (not linear, but cubic) equations with $(n-1)\times(m-1)$ indeterminate values of f in the interior mesh points:

$$\begin{aligned}&\left(4h^2+\left(f_{i+1,j}-f_{i-1,j}\right)^2\right)\left(f_{i,j+1}-2f_{i,j}+f_{i,j-1}\right)+\\&+\left(4k^2+\left(f_{i,j+1}-f_{i,j-1}\right)^2\right)\left(f_{i+1,j}-2f_{i,j}+f_{i-1,j}\right)-\\&-\frac{1}{2}\left(f_{i+1,j}-f_{i-1,j}\right)\left(f_{i,j+1}-f_{i,j-1}\right)\left(f_{i+1,j+1}-f_{i-1,j+1}-f_{i+1,j-1}+f_{i-1,j-1}\right)=0\end{aligned} \tag{13}$$

However, due to original discretization, this nonlinear system transforms easily into iterative process

$$\begin{aligned}f_{i,j} \;=\; &\frac{1}{2\left(4h^2+\left(f_{i+1,j}-f_{i-1,j}\right)^2\right)+2\left(4k^2+\left(f_{i,j+1}-f_{i,j-1}\right)^2\right)}\times\\&\times[\left(4h^2+\left(f_{i+1,j}-f_{i-1,j}\right)^2\right)\left(f_{i,j+1}+f_{i,j-1}\right)+\left(4k^2+\left(f_{i,j+1}-f_{i,j-1}\right)^2\right)\left(f_{i+1,j}+f_{i-1,j}\right)-\\&-\frac{1}{2}\left(f_{i+1,j}-f_{i-1,j}\right)\left(f_{i,j+1}-f_{i,j-1}\right)\left(f_{i+1,j+1}-f_{i-1,j+1}-f_{i+1,j-1}+f_{i-1,j-1}\right)]\end{aligned} \tag{14}$$

where, in order to find the value in one mesh point, the eight neighbouring mesh points are being used (four horizontal and vertical, but also four diagonal points). Although this is in the spirit of the method used in [2] and elsewhere (the Newton iteration with relaxation parameter), this one is different: it is a non-linear, non-Newton iteration method.

As the initial value $f^{(0)}$ for f in the iterative process we take the solution of the Laplace's equation

$$f_{xx}+f_{yy}=0 \tag{15}$$

with the same boundary condition. Using the same central difference formulas, this equation linearizes to a simple linear system in the standard iterative form

$$f_{ij}=\frac{1}{4}\left(f_{i+1,j}+f_{i-1,j}+f_{i,j+1}+f_{i,j-1}\right). \tag{16}$$

In calculated examples we use linear boundary conditions (BC). If the value $f(x,y)$ is interpreted as the height of the spatial point over $(x,y)\in B$, the BC are visualized as space quadrilateral $Q=\{(x,y,f(x,y)):(x,y)\in B\}$.

4. Results

The first model example is an asymmetric patch over the domain $U=(-1,1)\times(-1,1)$ with different heights of $z=8$ and $z=16$ over the opposite corners (and height $z=0$ in the two other corners), divided into rectangular mesh with $n=m=21$. Programming the process described in Section 3 in the package Mathematica®, we establish that it converges to a solution of the original minimal surface equation. The initial approximation $f^{(0)}$ (the solution of the Laplace's equation) is obtained in 761 iterations with iteration precision of $\varepsilon=10^{-5}$. As expected, it is a hyperbolic-paraboloidal patch.

On *Fig. 3* the minimal surface f obtained by the iterative process starting with $f^{(0)}$ is shown, obtained in 427 iterations with iteration precision of $\varepsilon=10^{-5}$. The maximum of the difference between $f^{(0)}$ and f over the given domain is $\max_U\left|f-f^{(0)}\right|=0.2390$. The graphical representation of this difference is practically the same as in *Fig. 5* below. The solution f should be regarded as the exact minimal surface according to given boundary conditions.

Using the commercial software EASY®, produced by Technet GmbH for form-finding in the same example setting with the same boundary conditions without external loads,the surface g is obtained. This

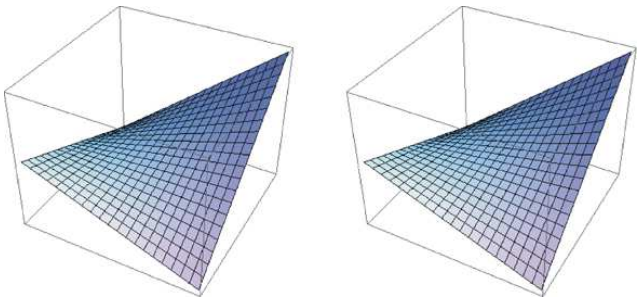

Figure 3: The initial approximation $f^{(0)}$ (left) and the minimal surface f (right)

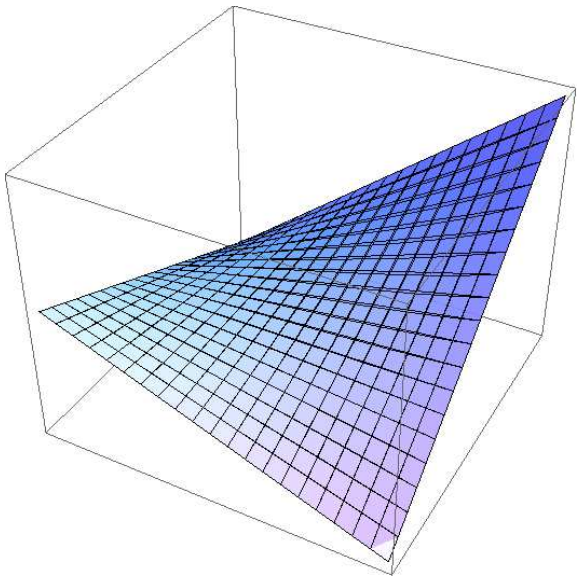

Figure 4: The minimal surface f and the surface g obtained by EASY®

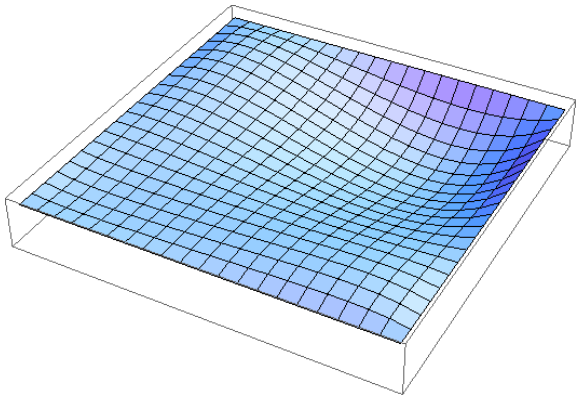

Figure 5: The difference $f - g$.

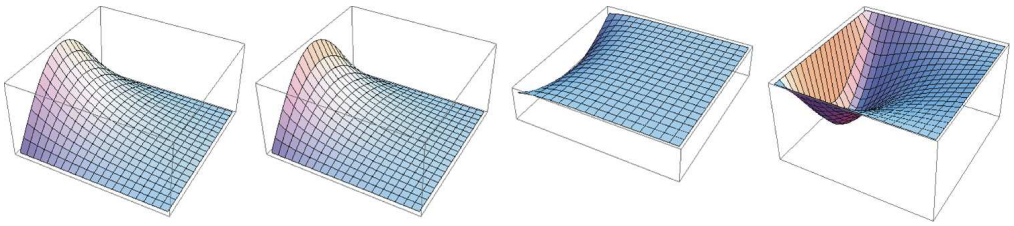

Figure 6: Example from [2] (left to right): $f^{(0)}$, f, mean curvature of $f^{(0)}$ and $f - f^{(0)}$.

surface is practically the same as our initial surface $f^{(0)}$ (see *Fig. 3* left) obtained by solution of the Laplace's equation, the maximum difference of the two over the given domain being $\max_U \left|g - f^{(0)}\right| = 0.00789$.

Fig. 4 shows both the minimal surface f and the surface g found by EASY® on the same graph. As it is seen, there are differences between this solution and the minimal surface solution, which can be noted especially in the region close to the higher corner.

The next *Fig. 5* shows the difference between the minimal surface f found by our method and the surface g, multiplied by factor 10.0 for visibility. The maximum difference of the two solutions over the given domain is $\max_U \left|f - g\right| = 0.23942$. This amounts approximately to 1.50% of the height.

The second example is the model example from [2]. The only non-zero boundary line is the sinusoidal arc. The initial approximation $f^{(0)}$ (the solution of the Laplace's equation) is obtained in 670 iterations with iteration precision of $\varepsilon = 10^{-5}$, and the minimal surface f in 620 iterations with the same precision. The maximum of the difference between $f^{(0)}$ and $f$over the given domain is $\max_U \left|f - f^{(0)}\right| = 0.1990$. The graphical representation of $f^{(0)}$, f, the mean curvature of $f^{(0)}$ (which is not zero since this is not a minimal surface) and the difference between $f^{(0)}$ and f multiplied by factor 10.0 are shown in *Fig. 6*.

In the third example we changed the boundary condition in order to have two sinusoidal arcs on two opposite sides - a saddle-like structure. The initial approximation $f^{(0)}$ (the solution of the Laplace's equation) is obtained in 726 iterations with iteration precision of $\varepsilon = 10^{-5}$, and the minimal surface f in 761 iterations with the same precision. The maximum of the difference between $f^{(0)}$ and f over the given domain is $\max_U \left|f - f^{(0)}\right| = 0.2011$. The corresponding graphical representations are shown in *Fig. 7*.

As the last example we used one-point fixed support in the centre of the patch (tent-like structure). In this singular case (the boundary consists of a closed line and an interior fixed point at the centre), our approach is not applicable, and the Laplace's equation solution gives a more plausible result (570 iterations, $\varepsilon = 10^{-5}$, *Fig. 8* left), while the minimal surface solution (719 iterations, $\varepsilon = 10^{-5}$, *Fig. 8* right) tends to become flat and singular with one-point discontinuity.

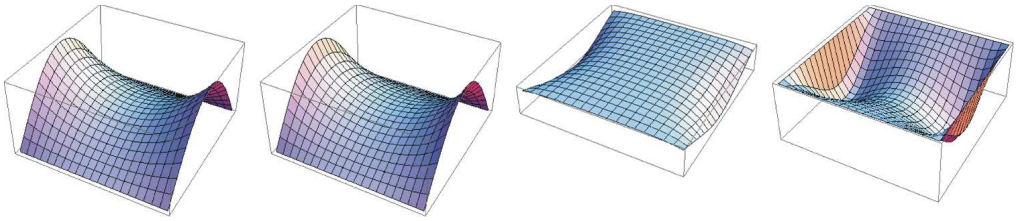

Figure 7: A saddle-like structure with sinusoidal boundaries (left to right): $f^{(0)}$, f, mean curvature of $f^{(0)}$ and $f - f^{(0)}$.

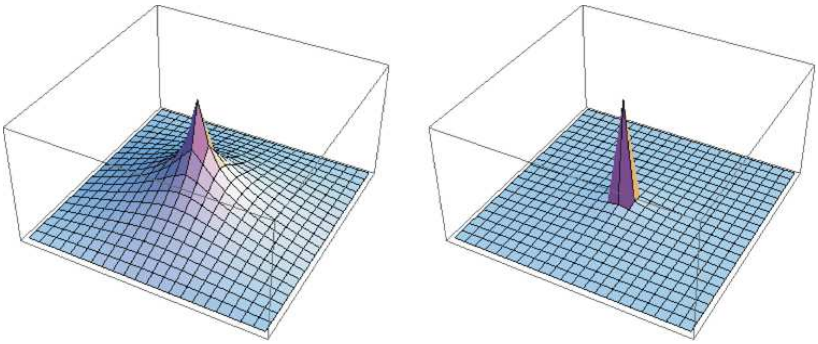

Figure 8: The case of singular boundary.

5. Conclusion

The standard model of the soap film surface developed in architecture by Frei Otto led to a widely spread belief that the best architectural solution for tensile structures is the minimal surface. In the present paper, a simple iterative nonlinear process which can be used to obtain the exact minimal surface over a fixed given quadrilateral domain is described. The commercial software used for the same purpose as its output usually does not give the minimal surface but the surface which corresponds to the solution of the Laplace's equation. Four analyzed examples are shown: the asymmetric hyperboloidal patch, the Concus' sine arc example, the modified saddle-like structure example and the tent-like structure with singular boundary. The difference of the two approaches did not exceed 1.50% of the height. Under standard exploiting conditions, this does not consist a notable difference. Under heavy load circumstances, the difference might be considered notable. The simple finite-difference approach with rectangular elements described above does not, however, possess the flexibility of the finite-element approach (triangular elements etc.) with flexible boundary conditions, used in the commercial software. It is also not suitable in the case of singular boundary, as the last example shows.

References

[1] R. Osserman, A Survey of Minimal Surfaces, Dover Publ, NY, 2002.
[2] P. Concus, Numerical Solution of the Minimal Surface Equation, Math Comput 20 (1967) 340–350.
[3] F. Otto, B. Rasch, Finding Form - Towards an Architecture of the Minimal, Edition Axel Menges, 1996.
[4] H. Berger, Light structures, structures of light: The art and engineering of tensile architecture, Birkhäuser Verlag, 1996.
[5] K. Bach, B. Burkhardt, F. Otto, IL 18 – Seifenblasen, Forming Bubbles, Krämer Stuttgart, 1988.
[6] D. Veenendaal, Ph. Block, An Overview and Comparison of Structural Form Finding Methods for General Networks, Int J Solids Structures 49 (2012) 3741–3753.
[7] R. Höller, FormFindung: architektonische Grundlagen für den Entwurf von mechanisch vorgespannten Membranen und Seilnetzen, Balistier Mähringen, 1999.
[8] Z. Zellinger, Zur Formfindung, Berechnung und Konstruktion von Membrantragwerken, Verlag der Techn Univ, Graz, 2005.
[9] D. Ströbel, P. Singer P, Computational Modelling of Lightweight Structures – Formfinding, Load Analysis and Cutting Pattern Generation; www.technet-gmbh.com

[10] 1 J. Lipkovski, Form-finding and Modeling of Membrane Structures based on Minimal Surfaces, Master thesis, University of Belgrade - Faculty of Civil Engineering, 2013.
[11] H.-J. Schek, The force density method for form finding and computation of general networks, Computer methods in applied mechanics and engineering, 3 (1974) 115–134.
[12] M.R. Barnes, Form finding and analysis of tension space structure by dynamic relaxation, PhD Thesis, Department of Civil Engineering, The City University, London, 1977.